The Astrophysical Journal, 624:821–826, 2005 May 10

AN EXTENDED SEARCH FOR CIRCULARLY POLARIZED INFRARED RADIATION FROM THE OMC-1 REGION OF ORION

M. Buschermöhle[1] and D. C. B. Whittet
Department of Physics, Applied Physics and Astronomy, and New York Center for Studies on the Origins of Life (NSCORT), Rensselaer Polytechnic Institute, 110 8th Street, Troy, NY 12180

A. Chrysostomou, J. H. Hough, and P. W. Lucas
Department of Physical Sciences, University of Hertfordshire, Hatfield, AL10 9AB, UK

A. J. Adamson
Joint Astronomy Center, 660 North A'ohoku Place, University Park, Hilo, HI 96720

and

B. A. Whitney and M. J. Wolff
Space Science Institute, 4750 Walnut Street, Suite 205, Boulder, CO 80301
Received 2004 September 22; accepted 2005 January 20

ABSTRACT

We present new observations of circular polarization (CP) at 2.2 μm in the Orion (OMC-1) molecular cloud. Our results extend a previously published study of the region. We show that the degree of CP correlates spatially with the molecular cloud and appears to be generally very low in regions dominated by H II. We detect a feature with 3%–5% CP that extends approximately 60″ to the southwest of the BN/IRc2 region. Although the morphology of the observed CP is broadly consistent with a model in which radiation from a central source (probably IRc2) is scattered by aligned spheroidal grains, we conclude that dichroic extinction in the foreground molecular cloud also plays a major role in its production. Implications of our results for the hypothesis that CP radiation imposes chiral asymmetry upon prebiotic organic molecules in protoplanetary disks are discussed. Mechanisms invoked to explain the observed CP in the near infrared can also produce CP in the range of ultraviolet wavelengths capable of chiral selection by photolysis; however, the polarized flux is likely to be of limited spatial extent and to have lower percentage CP compared with the infrared.

Subject headings: dust, extinction — infrared: ISM — ISM: individual (OMC-1) — ISM: magnetic fields — polarization

Online material: color figures

1. INTRODUCTION

Polarimetric observations of star formation regions are important for a number of reasons. They provide information on magnetic field structure, grain alignment, and other properties of the dust grains in molecular clouds and on the morphology of young stellar objects (YSOs) and their disks and outflows. At near-infrared wavelengths, partial plane polarization may result from scattering (in reflected radiation) or from dichroism (i.e., dichroic extinction in the transmitted beam from a background source observed through a medium of aligned grains). Circular polarization (CP) is produced in cases of multiple scattering, scattering of linearly polarized radiation, scattering of unpolarized radiation by aligned aspherical grains, or dichroism involving multiple clouds or twisted magnetic field lines. While linear polarization (LP) is observed ubiquitously in the environs of both low- and high-mass stars (e.g., Bastien 1996), observations of CP are as yet less common.

An important motivation for studies of CP in regions of active star formation is the possibility that photolytic processes involving CP might provide a viable mechanism for chiral selection of biologically significant molecules (e.g., Bonner 1991; Bailey 2001, 2004; Meierhenrich & Thiemann 2004). A chiral molecule possesses two possible configurations that are chemically equivalent but differ physically in that they are mirror images of each other. A characteristic signature of biological systems on Earth is the preference for molecules of a single chiral form (enantiomers); i.e., terrestrial life is "homochiral": proteins are composed of left-handed (L) amino acid monomers, while nucleic acids contain right-handed (D) sugars. In contrast, organic matter produced by nonbiological processes is generally racemic, i.e., the L and D forms of chiral molecules are present in roughly equal numbers. The origin of terrestrial homochirality is unknown. However, detection of significant L-enantiomeric excesses in meteoritic α-methyl amino acids (Cronin & Pizzarello 1997, 1999; Pizzarello & Cronin 2000; Pizzarello 2004) suggests that this phenomenon might be intimately linked with the origin of the solar system itself and its star formation environment. If this excess were a general feature of the solar nebula, it would have been present in the material delivered to Earth during the late accretion phase of planet formation. Amino acids have been synthesized in laboratory analog experiments that simulate ultraviolet (UV) photolysis of interstellar ices (Bernstein et al. 2002; Muñoz Caro et al. 2002). If the incident radiation is circularly polarized, an enantiomeric excess may arise from asymmetric photochemical synthesis, or from asymmetric photolysis in which one enantiomer is preferentially destroyed, as has been demonstrated in the laboratory for a variety of interesting biomolecules (Balavoine et al.

[1] Current address: Institut für Chemie und Biologie des Meeres, Carl von Ossietzky Universität Oldenburg, D-26111 Oldenburg, Germany.

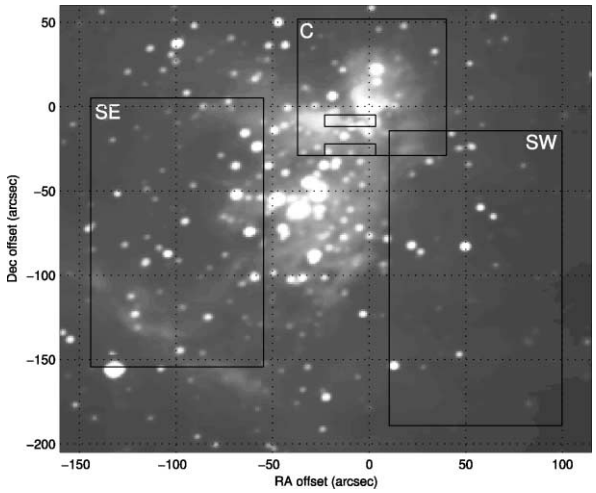

FIG. 1.—Areas of OMC-1 observed in CP, superposed on a *K*-band intensity image of the region from 2MASS. North is to the top, and east is to the left. The square above center (labeled C) designates the area observed by Chrysostomou et al. (2000). All offsets are relative to the position of the BN object (R.A. = $05^h35^m14^s.5$, decl. = $-05°22'22''$, J2000). The two main fields observed in the present work are centered to the southwest (SW) and southeast (SE) of BN. The SW field is located between R.A. = $05^h35^m13^s$, decl. = $-05°22'36''$ (*upper left corner*) and R.A. = $05^h35^m07^s$, decl. = $-05°25'18''$ (*lower right corner*); the SE field is located between R.A. = $05^h35^m24^s$, decl. = $-05°22'15''$ (*upper left corner*) and R.A. = $05^h35^m18^s$, decl. = $-05°25'01''$ (*lower right corner*); (all are J2000 coordinates). Two smaller rectangular areas observed in the present work that lie entirely within area C are also shown. [*See the electronic edition of the Journal for a color version of this figure*.]

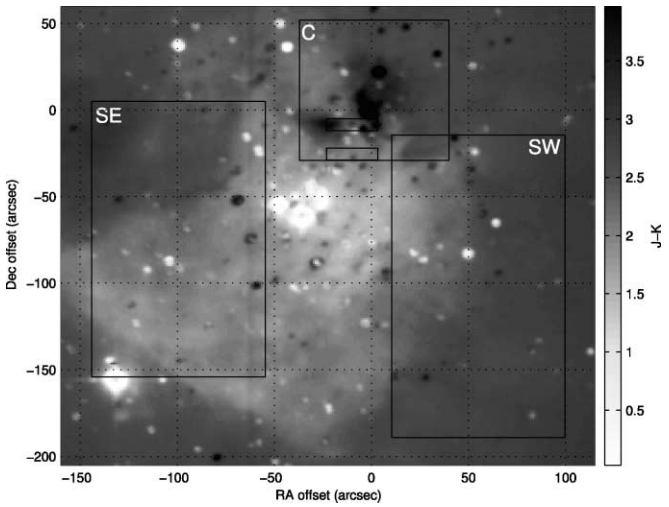

FIG. 2.—Similar to Fig. 1, but with a 2MASS $J - K$ color image underlying the selected areas. The point sources near the center of the image are members of the Trapezium cluster. The dark area to the northwest of the Trapezium is a region of high extinction centered near the BN object. [*See the electronic edition of the Journal for a color version of this figure*.]

1974; Flores et al. 1977; Norden 1977; Greenberg et al. 1994; Meierhenrich & Thiemann 2004). Greatest yields typically occur for radiation in the 200–230 nm region of the spectrum. Even a small enantiomeric excess introduced in this way might prove significant, as amplification via asymmetric autocatalysis has been shown to be efficient in the laboratory (Shibata et al. 1998).

Because of high dust extinction, observations of CP in star formation regions are not generally feasible in the UV. Observations at longer wavelengths indicate that high levels of CP ($\sim$10% or more) are present in the near-infrared in at least two regions containing massive YSOs: OMC-1 (Bailey et al. 1998; Chrysostomou et al. 2000) and NGC 6334 (Ménard et al. 2000), while more modest levels of up to a few percent are typical of lower mass objects (e.g., Gledhill et al. 1996; Clark et al. 2000; Clayton et al. 2005). Models suggest that scattering by aligned aspherical grains, dichroic extinction, or some combination of the two are the only mechanisms capable of explaining the highest observed levels of CP (Chrysostomou et al. 2000; Whitney & Wolff 2002; Lucas 2003; Lucas et al. 2005). There is, of course, no guarantee that CP will be present at UV wavelengths in regions where infrared CP is observed, but calculations by Lucas et al. (2005) do suggest that when a UV flux is present, it may exhibit substantial levels of CP.

Regions of massive star formation inevitably become exposed to intense UV irradiation as the stars they produce evolve. A substantial interaction between the UV photon field and ambient interstellar dust is indicated, for example, by the detection of molecules, such as nitriles or cyanates, that most likely formed by photochemical reactions in grain mantles (Whittet et al. 2001 and references therein). Subsequent evaporation of the mantles may lead to further chemical processing of organic molecules in the gas phase (e.g., van Dishoeck & Blake 1998). In such environments, the CP flux needed for production of a significant enantiomeric excess in amino acids ($\sim 1.8 \times 10^{17}$ UV photons cm^{-2}, according to Greenberg et al. 1994) may be reached in only $\sim$2000 yr (Bailey et al. 1998); i.e., in timescales that are short compared with those for dynamic evolution of protoplanetary disks. If the CP model is broadly correct, chiral asymmetry may be relatively common in low-mass systems that form in close proximity to high-mass stars.

The purpose of this paper is to present new observations of near-infrared CP in the Orion molecular cloud (OMC-1). Our observations (§ 2) extend the previous CP imaging presented by Chrysostomou et al. (2000) to cover two additional areas that contain low-mass members of the Orion Nebular cluster centered on the Trapezium group (see, for example, Muench et al. 2002). Our results provide additional insight into the nature of environments that lead to efficient CP production. Implications are discussed in § 3 and our conclusions are summarized in § 4.

2. OBSERVATIONS AND DATA REDUCTIONS

Two rectangular areas adjacent to the central area of OMC-1 mapped by Chrysostomou et al. (2000) were selected for observation. These were observed on the nights of 2003 March 1 and 2 (UT) with the Fast-Track Imager (UFTI) and infrared polarimeter (IRPOL2) on the United Kingdom Infrared Telescope (UKIRT) at Mauna Kea Observatory, Hawaii. The imager uses a 1024×1024 pixel HgCdTe array. All observations were taken in the standard *K* (2.2 μm) passband. The regions selected for observation are shown overlaid on *K*-band intensity and $J - K$ color images from the Two Micron All Sky Survey (2MASS) in Figures 1 and 2 (respectively). All offsets are relative to the position of the BN object in OMC-1. For convenience, we refer to our selected areas by position (southwest and southeast, hereafter SW and SE) relative to the BN object, and we designate the area studied by Chrysostomou et al. (2000) by the letter C. Note that Chrysostomou et al. used a different telescope (the Anglo Australian Telescope) and instrumentation. One of our selected areas (SW) overlaps C, allowing a check for consistency. In addition, we also report here previously unpublished *K*-band

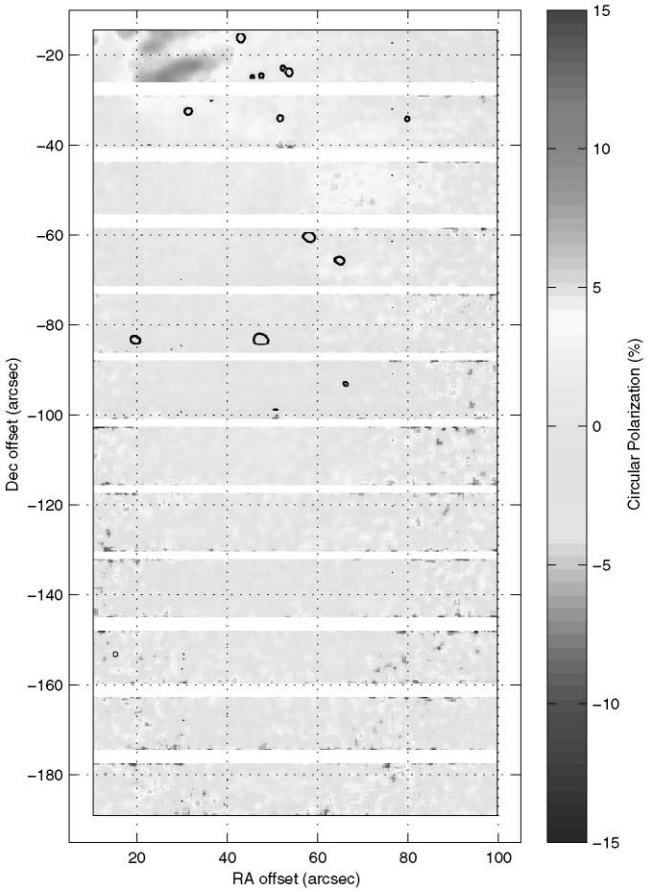

FIG. 3.—Final CP map of the SW area. Superposed intensity contours indicate the positions of bright *K*-band point sources. [*See the electronic edition of the Journal for a color version of this figure.*]

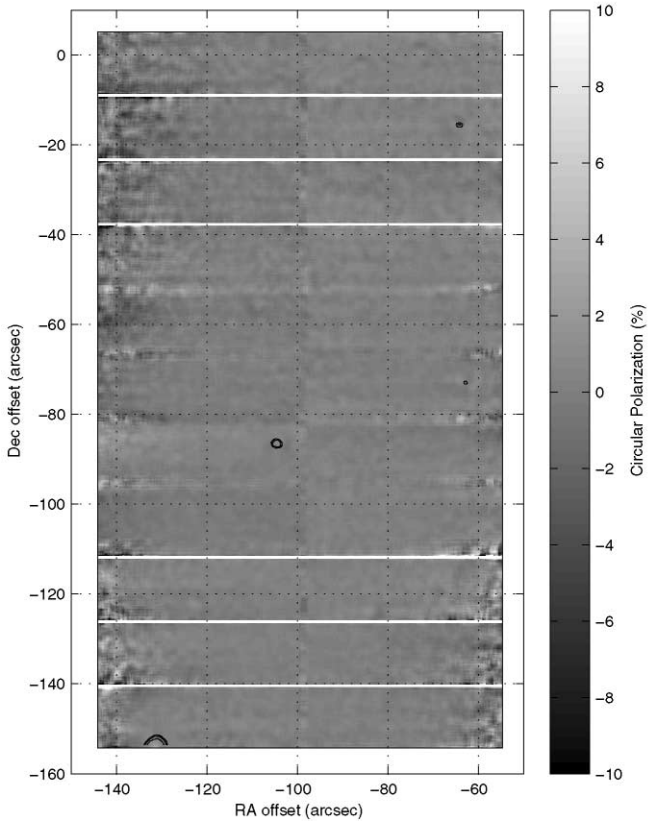

FIG. 4.—Similar to Fig. 3 but for the SE area. [*See the electronic edition of the Journal for a color version of this figure.*]

observations, obtained with UKIRT on 1999 January 5 (UT), of two narrow strips entirely within area C (see Fig. 1). In this case, the imaging system used was IRCAM3 with a 256×256 pixel array.

IRPOL2 is a dual-beam polarimeter built at the University of Hertfordshire. A quarter-wave plate external to the cryostat is used with a beam-splitting Wollaston prism, inside the cryostat, to act as the analyzer and produce separate *o*- and *e*-ray images, which are then combined to give CP. A half-wave plate is spun continuously in front of the stepped quarter-wave plate: this is very effective in ensuring that a negligible amount of the very high LP present is measured as CP. Data reductions were carried out using the procedure described by Chrysostomou et al. (2000). For the 2003 March run, each selected area was covered by several sets of images, each of which contained two *o*- and *e*-beam slices within a $93'' \times 70''$ field. One set consisted of eight images, each with a 30 s integration time: four data images at analyzer position angles of 0°, 45°, 90°, and 135°, and four offset sky images at the same angles. The corresponding sky frame was subtracted from the data frame for each analyzer angle, and the *I* and *V* Stokes parameters were calculated from the *o*- and *e*-beam intensities for pairs of images with analyzer angles differing by 90° (see Chrysostomou et al. 2000 for details). Each selected area was covered by a series of image sets separated by $15''$ in declination. Although in principle a single slice had a height of $23''$, in practice only about $13''$ was used in the reduction, owing to the onset of partial vignetting at the edges of the polarimetry aperture mask; because of this, the slices usually do not overlap. The pixel size in the final CP images is $0\farcs18 \times 0\farcs18$ for UFTI IRPOL2 data. The IRCAM3 observations were obtained and reduced using an analogous procedure: three 10 s exposures were combined to yield final images in two $27'' \times 5''$ strips within area C, with a pixel size of $0\farcs14 \times 0\farcs14$.

Because CP is calculated from intensity ratios, the observational error is a strong function of intensity. The standard deviation for an individual pixel in our raw images is typically ± 2 (percent CP) in regions of high intensity (e.g., close to BN), rising to as much as ± 10 in regions of low intensity. The final maps, presented in Figures 3–5, have been smoothed by averaging over a 9×9 pixel square centered on each pixel in the image. This reduces the typical error in percentage CP to ± 1 or better over essentially the entire surveyed area.

3. RESULTS AND DISCUSSION

CP maps from our observations are presented in Figures 3, 4, and 5 for areas SW, SE, and C, respectively; in addition, Figure 6 presents an overview map of all three areas superposed on a *K*-band intensity contour map. Our results are in good agreement with the previously published map of Chrysostomou et al. (2000) in areas of overlap. The overlap includes a highly circularly polarized ($\sim$12%) region in the northeastern corner of the SW area (Fig. 3) and regions of both high and low polarization in the additional observations of area C (Fig. 5).

The most striking result of our work is that the amplitude of CP at 2.2 μm is generally low ($\pm 1\%$ or less) in the outlying regions of OMC-1 included in our survey. The SW area includes a feature with 3%–12% CP that extends some $60''$ southwest

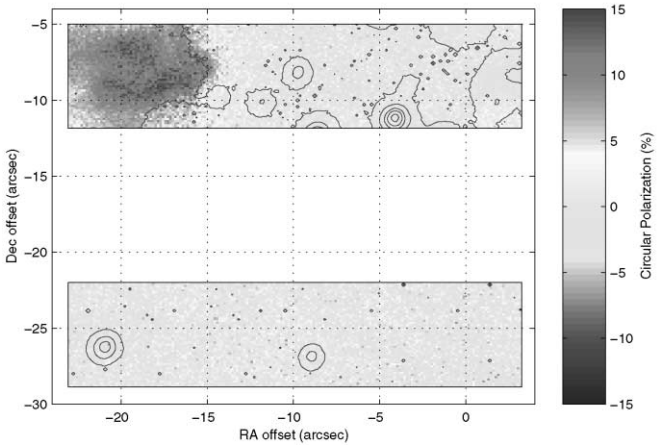

FIG. 5.—CP of two strips in area C from the 1999 January observing run. *K*-band intensity contours are superposed. [*See the electronic edition of the Journal for a color version of this figure*.]

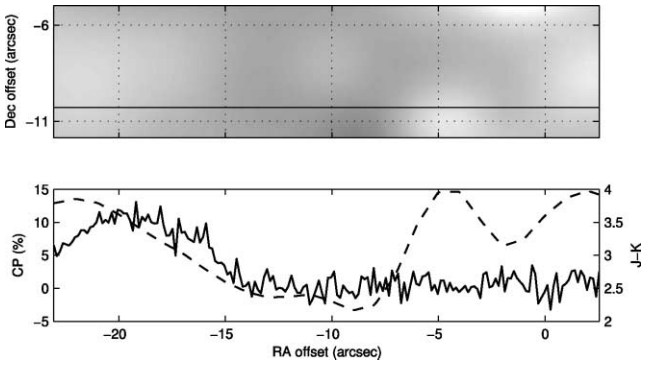

FIG. 7.—Comparison of $J - K$ color and CP for a sample cut through the northerly strip observed in area C. The upper frame shows the locus of the cut (*horizontal line*) on the $J - K$ image, and the lower frame plots CP (*continuous curve*) and $J - K$ (*dashed curve*) against R.A. offset along the cut. [*See the electronic edition of the Journal for a color version of this figure*.]

from area C, but the remainder of the region has CP close to zero. The SE area contains no discernible features, and again the mean background level is essentially zero, to within the uncertainty. Our results, in combination with those of Chrysostomou et al. (2000; their Fig. 1) strongly suggest that the highest CP levels (>5%) are generally confined to regions within $30''-40''$ of BN, i.e., toward the heart of the OMC-1 molecular cloud. This region is characterized by relatively large $J - K$ color (the darker areas in Fig. 2). If the intrinsic background were uniform, then $J - K$ would measure the reddening by dust, and hence the total extinction for an assumed extinction law. Although gradients are likely to be present in the intrinsic background, $J - K$ is probably a reasonable guide to extinction in localized regions away from point sources.

To illustrate the correlation of CP with $J - K$, we compare in Figures 7 and 8 the behavior of these quantities in two sample regions. CP amplitude and $J - K$ are plotted against R.A. offset ($\Delta\alpha$) along lines of constant declination, for a cut through the northerly strip observed in area C (Fig. 7) and through the extended feature in the northerly part of the SW area (Fig. 8). In each case, the locus of the cut is shown on the $J - K$ image in the upper frame. Of greatest interest in Figure 7 is the corresponding rise in both CP and $J - K$ in the nebulosity to the east of BN, in the range $-20 < \Delta\alpha < -8$. (Note that $J - K$ is affected by point sources at $\Delta\alpha \approx +2$ and -4.) There is also evidence of correlated behavior in the SW feature (Fig. 8).

As noted in § 1, only two mechanisms, scattering from aligned grains and dichroic extinction, appear capable of producing the highest observed levels of CP. Insight into which of these dominates may be obtained by comparing the spatial distribution of extinction (as inferred from $J - K$ color; our Fig. 2) with those of both CP and LP in region C (see Fig. 7 of Chrysostomou et al. 2000). We discuss each mechanism in turn.

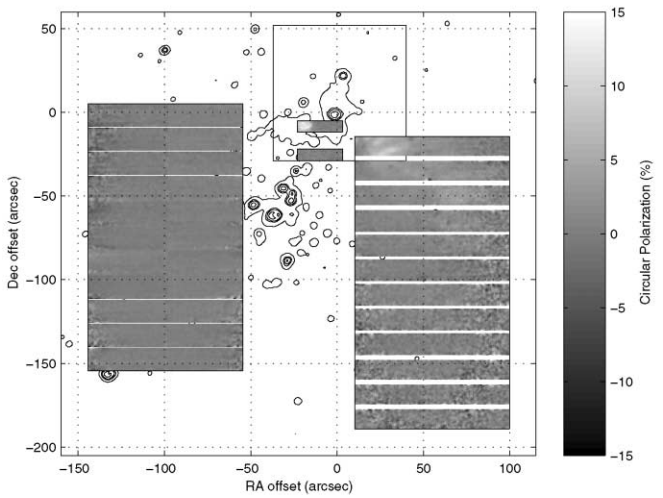

FIG. 6.—Overview of results from Figs. 3–5, superposed on a 2MASS *K*-band intensity contour map. [*See the electronic edition of the Journal for a color version of this figure*.]

3.1. *Scattering from Aligned Grains*

The CP observed in the BN/IRc2 region displays quadrupolar morphology, which led Chrysostomou et al. (2000) to propose a model that incorporates scattering of radiation from a central source by spheroidal grains aligned by the local magnetic field. Such morphology is produced routinely in radiation transfer models of protostellar envelopes that include scattering from aligned oblate or prolate grains with axial ratios ~2:1 and for any viewing angle that is not close to pole-on (Gledhill & McCall 2000; Whitney & Wolff 2002). The observed structure suggests that IRc2 (located $\sim 9''$ southeast of BN) is the most probable illuminating source. Regions of highest CP are presumed to be physically separate from the associated outflow (which would disrupt grain alignment) and to have a relatively unobscured view of the illuminating source. This is consistent with the observed CP: for example, the extended feature in our SW area (Figs. 3 and 6) has orientation approximately orthogonal to the outflow (see Schild et al. 1997) and approximately radial to IRc2. Regions of high CP in OMC-1 also exhibit high LP, but the converse is not true, in agreement with scattering models.

3.2. *Dichroic Extinction*

Although scattering models explain the morphology of the observed CP, general confinement of the highest levels to regions of large $J - K$ reddening strongly suggests that dichroic extinction also plays an important, perhaps dominant, role. Dichroic extinction by a screen containing uniformly aligned grains introduces LP to an initially unpolarized incident beam. However, if the incident beam is already linearly polarized (e.g., because of prior dichroic extinction or scattering) or if the direction of alignment changes systematically (e.g., because of

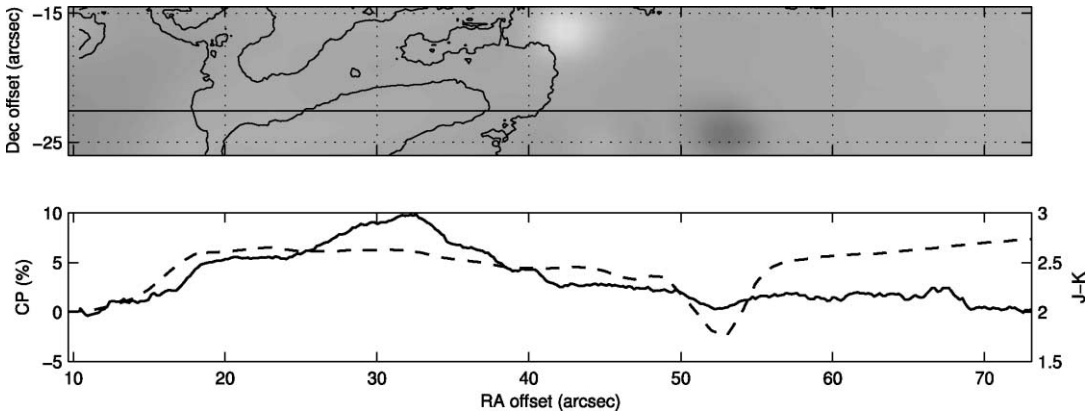

FIG. 8.—Similar to Fig. 7, but for a cut through the northerly part of the SW area. [*See the electronic edition of the Journal for a color version of this figure.*]

twisted magnetic field lines), then CP is also produced (effectively by conversion of Stokes U to Stokes V by birefringence; Martin 1974; Whitney & Wolff 2002; Lucas et al. 2005). The highest observed levels of CP (>12%) can be explained by oblate grains with axial ratios ~1.5:1 (Lucas et al. 2005), consistent with predictions based on laboratory analog experiments involving particle aggregation (Wurm & Blum 2000). The observed CP amplitude also depends on the magnetic field direction relative to the line of sight, which may explain the fact that CP is not always high when $J - K$ reddening is high (Figs. 7 and 8).

A further argument in favor of dichroic extinction concerns the observed wavelength dependences of CP, LP, and ellipticity (the ratio of CP to LP). These are tabulated for the high-CP region southeast of BN for three wavelengths (1.6, 2.2, and 3.8 μm) in Table 2 of Chrysostomou et al. (2000). For sub-micron-sized dielectric grains, scattering models predict that CP and ellipticity both increase monotonically with decreasing wavelength through the near infrared, up to a peak in the visible. While the observed ellipticity does, indeed, rise monotonically, CP drops sharply at 1.6 μm compared with 2.2 μm. By contrast, for dichroic extinction, the peak in CP at 2.2 μm can be explained by the competing and opposite wavelength dependences of LP and birefringence. Models show that birefringence rises with decreasing wavelength in the near-infrared (Martin 1974), while the observed LP falls rapidly with decreasing wavelength in a manner consistent with scattering by grains with a scattering angle approximately in the range 45°–70° (see Lucas et al. 2005). Hence, for dichroic extinction, we expect CP to be low at shorter infrared wavelengths, because LP is low (there is not much LP to convert to CP), while ellipticity should rise with the wavelength dependence of birefringence, as it does.

3.3. *Implications for CP in the Ultraviolet*

Both of the above mechanisms can, in principle, produce high CP at the mid-UV wavelengths needed to drive chiral selection of prebiotic molecules. However, because of the much higher optical depth of the medium in the UV, high CP is likely to be confined to a relatively small region near the embedded source of luminosity. Moreover, the circularly polarized component of the ambient radiation field is likely to be lower in the UV compared with the near infrared, because the UV phase function of sub-micron-sized grains is highly forward throwing (see Lucas et al. 2005). This implies that only a small fraction of radiation will be scattered through the large angles required to produce high CP by scattering from aligned grains. CP production by dichroic extinction will also be compromised, if scattering is the primary means of producing the initial LP (converted to CP by birefringence): although high LP can occur at large scattering angles in the UV, its flux will be small and may be diluted by other sources of radiation.

As noted in § 3.2 above, the birefringence of a mixture of sub-micron-sized dielectric grains is expected to rise with decreasing wavelengths from the infrared to the visible. It may reach a plateau in the visible to UV, or even decline if small, absorptive, carbonaceous particles provide a significant fraction of the dust opacity, as suggested by some interstellar grain models. Since the opacity of the medium rises as the wavelength declines, the birefringence per unit optical depth is predicted to be much lower in the UV than in the infrared. Hence, the CP produced by dichroic extinction can only be high in regions where the radiation field passes through a fairly high optical depth, thus further reducing the available flux for photolysis. High optical depth also leads to increased multiple scattering, which tends to reduce the percentage of CP. These factors may explain why Clayton et al. (2005) find only upper limits (<1%) on CP amplitude in the V and I passbands toward several YSOs of intermediate to high mass.

In summary, CP may be significant at UV wavelengths in the vicinity of embedded high-mass YSOs, such as IRc2 in OMC-1, but for several reasons the polarized flux is likely to be lower than in the infrared. Because the flux required for significant asymmetric photolysis is not tightly constrained, it is difficult to make a quantitative prediction of how much matter in the system might be sufficiently irradiated for a significant enantiomeric excess to arise in any chiral molecules it contains. Further progress is likely to require both more laboratory work, to better determine how much flux is required to produce significant enantiomeric excesses in molecules of biological interest, and more observations of CP in a variety of star formation environments.

4. CONCLUSIONS

We have extended previously published maps of circularly polarized radiation at 2.2 μm in OMC-1. We show that CP correlates spatially with reddening in the molecular cloud (as measured by the $J - K$ color index) and appears to be generally very low in lines of sight toward the H II region lacking dense molecular material. A feature with 3%–5% CP is detected that extends ~60″ to the southwest from the BN/IRc2 region. Although the morphology of the observed CP is consistent with a model in which radiation from a central source (probably IRc2) is scattered by aligned spheroidal grains, we conclude that dichroic extinction in the foreground molecular cloud also plays

an important (and perhaps dominant) role in its production. The CP flux available for UV photolysis of chiral molecules is likely to be of limited spatial extent and may have generally lower polarization amplitude compared with the infrared.

The New York Center for Studies on the Origins of Life is a NASA-funded Specialized Center for Research and Training. D. C. B. W. gratefully acknowledges additional support from the NASA Exobiology and Origins of Solar Systems programs (grants NAG 5-13469 and NAG 5-11662, respectively). The United Kingdom Infrared Telescope is operated by the Joint Astronomy Centre on behalf of the UK Particle Physics and Astronomy Research Council. IRPOL2 was built for UKIRT by the Department of Physical Sciences, University of Hertfordshire. We are grateful to James Ferris for comments on the manuscript and for stimulating discussions on the topic of chirality. We also acknowledge helpful comments from an anonymous referee.

REFERENCES

Bailey, J. 2001, Origins Life Evol. Biosphere, 31, 167
———. 2004, in IAU Symp. 213, Bioastronomy 2002: Life among the Stars, ed. R. P. Norris & F. H. Stootman (San Francisco: ASP), 139
Bailey, J., et al. 1998, Science, 281, 672
Balavoine, G., Moradpour, A., & Kagan, H. B. 1974, J. Am. Chem. Soc., 96, 5152
Bastien, P. 1996, in ASP Conf. Ser. 97, Polarimetry of the Interstellar Medium, ed. W. G. Roberge & D. C. B. Whittet (San Francisco: ASP), 297
Bernstein, M. P., Dworkin, J. P., Sandford, S. A., Cooper, G. W., & Allamandola, L. J. 2002, Nature, 416, 401
Bonner, W. A. 1991, Origins Life Evol. Biosphere, 21, 59
Chrysostomou, A., Gledhill, T. M., Ménard, F., Hough, J. H., Tamura, M., & Bailey, J. 2000, MNRAS, 312, 103
Clark, S., et al. 2000, MNRAS, 319, 337
Clayton, G. C., Whitney, B. A., Wolff, M. J., Smith, P., & Gordon, K. D. 2005, in ASP Conf. Ser., Astronomical Polarimetry: Current Status and Future Directions, ed. A. J. Adamson et al. (San Francisco: ASP), in press
Cronin, J. R., & Pizzarello, S. 1997, Science, 275, 951
———. 1999, Adv. Space Res., 23, 293
Flores, J. J., Bonner, W. A., & Massey, G. A. 1977, J. Am. Chem. Soc., 99, 3622
Gledhill, T. M., Chrysostomou, A., & Hough, J. H. 1996, MNRAS, 282, 1418
Gledhill, T. M., & McCall, A. 2000, MNRAS, 314, 123
Greenberg, J. M., et al. 1994, J. Biol. Phys., 20, 61
Lucas, P. W. 2003, J. Quant. Spectrosc. Radiat. Transfer, 79, 921
Lucas, P. W., Hough, J. H., Bailey, J., Chrysostomou, A., Gledhill, T. M., & McCall, A. 2005, Origins Life Evol. Biosphere, in press
Martin, P. G. 1974, ApJ, 187, 461
Meierhenrich, U. J., & Thiemann, W. H. 2004, Origins Life Evol. Biosphere, 34, 111
Ménard, F., Chrysostomou, A., Gledhill, T. M., Hough, J. H., & Bailey, J. 2000, in ASP Conf. Ser. 213, Bioastronomy 99: A New Era in Bioastronomy, ed. G. A. Lemarchand & K. J. Meech (San Francisco: ASP), 355
Muench, A. A., Lada, E. J., Lada, C. J., & Alves, J. 2002, ApJ, 573, 366
Muñoz Caro, G. M., et al. 2002, Nature, 416, 403
Norden, B. 1977, Nature, 266, 567
Pizzarello, S. 2004, Origins Life Evol. Biosphere, 34, 25
Pizzarello, S., & Cronin, J. R. 2000, Geochim. Cosmochim. Acta, 64, 329
Schild, H., Miller, S., & Tennyson, J. 1997, A&A, 318, 608
Shibata, T., et al. 1998, J. Am. Chem. Soc., 120, 12157
van Dishoeck, E. F., & Blake, G. A. 1998, ARA&A, 36, 317
Whitney, B. A., & Wolff, M. J. 2002, ApJ, 574, 205
Whittet, D. C. B., Pendleton, Y. J., Gibb, E. L., Boogert, A. C. A., Chiar, J. E., & Nummelin, A. 2001, ApJ, 550, 793
Wurm, G., & Blum, J. 2000, ApJ, 529, L57